Multicomponent Fibers by Multi-interfacial Polyelectrolyte Complexation

Andrew C. A. Wan, Meng Fatt Leong, Jerry K. C. Toh, Yuangang Zheng, and Jackie Y. Ying**

Polyelectrolyte complexation is a chemical phenomenon that involves the formation of electrostatic bonds between two polyelectrolytes of opposite charges, leading to a stable macromolecular complex.[1,2] Due to its excellent material tunability, various modes of polyelectrolyte complexation leading to films,[2] multilayers,[3] and fibers[4] have been investigated. To enable spatially patterned cell co-culture within a fiber, this work investigated the fusing of fibers from multiple polyelectrolyte interfaces, which led to the observation of multi-interfacial polyelectrolyte complexation (MIPC). In MIPC, fusion of nascent fibers from multiple interfaces brought the interfaces to a point from which a single, fused composite fiber was drawn. We applied MIPC to two, three, and four polyelectrolyte complex interfaces to obtain various patterned multicomponent fibers. Cells encapsulated in these fibers exhibited migration, aggregation, and spreading in relation to the initial cell or matrix pattern, demonstrating the tremendous potential of MIPC for biological applications.

The self-assembly of polyelectrolyte complexes at an interface was first described by Yamamoto and co-workers in 1999.[4] Fibers can be drawn from the polyelectrolyte complex at the interface of two oppositely charged polyelectrolytes. With the aim of exploiting the advantage of this room-temperature, aqueous-based fiber processing for tissue engineering applications, Leong and co-workers, as well as our group, have adapted the technology for the encapsulation and delivery of biological molecules, such as proteins and DNA.[5–8] The interfacial polyelectrolyte complexation (IPC) process has also been investigated for potential biosensor and electronic applications.[9]

An important application of IPC fibers is in the area of tissue engineering,[10–13] whereby these fibers have been demonstrated to provide a conducive matrix for cell growth and differentiation. However, to emulate the structure and function of native tissue, more than one cell type is often required. While a co-culture may be achieved by simply encapsulating a mixture of cells, it has been demonstrated that a co-culture that involves pre-formed cell structures/domains leads to higher cell viability and function.[14,15] Furthermore, during embryogenesis, different cell types interact in the form of closely apposed layers. Accordingly, both homotypic interactions (between the same cell type) and heterotypic interactions (between different cell types) would be crucial for tissue development and in emulating native tissue structures.[16,17] Ideally, each cell type would be spatially defined and interacting within its own layer or domain, and each cell layer could then interact with cells from other layers. In theory, such multidomain or multicomponent fibers could be achieved by the fusion of IPC fibers at the right stage of the IPC process.

A multistep mechanism was proposed for IPC fiber formation, as shown in **Figures 1**a,b.[18] The first step is the formation of a polyelectrolyte complex fiber at the interface of two oppositely charged polymers (Plane I), which when drawn, leads to the formation of micrometer-sized "nuclear" fibers (Plane II). Subsequent growth and coalescence of the nuclear fibers (Planes III–IV) resulted in a "primary" fiber. We first asked ourselves whether the fibers could be fused at the solution-air interface, i.e. between Planes I and II of the IPC process. In theory, this would result in spatially defined components within the matrix of the combined fiber, each component arising from one interface (Figures 1c,d). While the basic polyelectrolyte constituents of the fiber would remain as a continuous matrix, the additional components (e.g. cells) that made up each domain would be defined in three-dimensional (3D) space.

Fusing fibers at the liquid-air interface entailed the drawing of fibers from interfaces in close proximity. The best way to achieve this would be to flank a droplet of polyelectrolyte solution with two droplets of the oppositely charged polyelectrolyte, to create two interfaces from which component fibers could be simultaneously drawn and fused (**Figure 2**a, Frames 1–2). However, this also presupposed that the layer of polyelectrolyte interceding between the flanking electrolytes would have to be minimal, which presented a practical difficulty. A surprising phenomenon was observed that circumvented the latter problem. When two nascent fibers arising from two interfaces of a three-droplet polyelectrolyte solution assembly (separated from each other by several millimeters) were fused by manual contact, the fibers were observed to zip down right to the air-liquid interface (Figure 2a, Frames 3–5). This zipping motion was due to the surface tension of the two wet fibers. Subsequently, a single fused fiber could be continuously drawn. In fact, manually contacting the nascent fibers to zip them together was not necessary when the interfaces were close enough to each other. Figure S1 (Supporting Information) shows how the fiber fusion event could occur spontaneously as the nascent fibers were being drawn out of the solution, resulting in the Y-shape fiber pattern characteristic of the process.

Figure 2b(I–III) illustrates the postulated movement and geometry of the three polyelectrolyte solutions. The fiber fusion event brings the flanking polyelectrolytes into close

Dr. A. C. A. Wan, Dr. M. F. Leong, J. K. C. Toh, Dr. Y. Zheng, Prof. J. Y. Ying
Institute of Bioengineering and Nanotechnology
31 Biopolis Way, The Nanos, Singapore 138669, Singapore
E-mail: awan@ibn.a-star.edu.sg; jyying@ibn.a-star.edu.sg

DOI: 10.1002/adhm.201100020

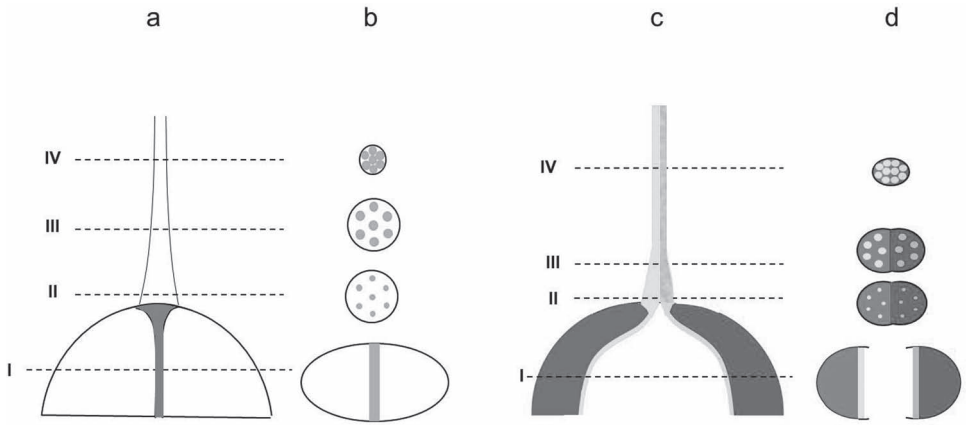

Figure 1. Mechanism of fiber formation by polyelectrolyte complexation at one interface: a) side view and b) plane view. I–IV denote the different planes of polyelectrolyte complex solutions and nascent fiber. Fusion of nascent fiber drawn from two polyelectrolyte complex interfaces at the solution-air interface would lead to two spatially defined components within the same fiber: c) side view and d) plane view. Green-white and red-white represent pairs of two oppositely charged polyelectrolyte solutions. In (b) and (d), the circles represent the nuclear fibers.

proximity, with each fiber drawing its respective interface to the midpoint above the droplet assembly. This hypothesis is supported by observing the movement of colored solutions (Figure 2a), and examining the dried polyelectrolyte complex interface (Figure 2c). The latter revealed a triangular layer of each flanking polyelectrolyte overlapping above the central polyelectrolyte of opposite charge.

MIPC is characterized by two other unique features. Firstly, the nascent fiber is observed to toggle at the solution-air interface, something not seen for the case of the single IPC (Supporting Information S2 and S3). Figures 2c (top view) and d (schematic side view) show two triangular layers of polyanions above and overlapping with the polycations droplet. During the drawing of MIPC fibers, these layers of polyanions were observed by microscopy to be easily shifted by movement of the fiber. As represented schematically in Figure 2b(III–V), the fused interface is observed to toggle laterally. The dynamic nature of the MIPC interface also allows the point from which the composite fiber leaves the fused interface to be shifted with a greater degree of freedom, in a manner defined by the direction of the drawing motion.

Secondly, while the fibers obviously fuse, the flanking polyelectrolytes do not mix and always remain as separate solutions. We attribute this to the streaming of the interceding polyelectrolyte to the interface, to replace the solution consumed by fiber drawing (Figure 2d). Thus, a dynamic layer of oppositely charged polyelectrolyte constantly intercedes between the two flanking polyelectrolyte solutions, creating a viscous polyelectrolyte complex mixture that precludes mixing. The important implication of this feature is that fiber can be drawn from two separate pools containing different components. In this way, the process retains the possibility of having spatially defined components within the composite fiber.

Similarly, MIPC fibers can be formed by the fusion of three or more interfaces. The additional interfaces can be achieved by adding droplets in series or in other defined patterns. For example, MIPC formation from four interfaces in series and the corresponding schematic representation is shown in Figures 2e and f. In this example, the two pairs of fibers on the outside were first fused, resulting in a pair of combined fibers (Figure 2e, Frame 3; Figure 2f(II)). The latter was then fused manually to achieve the final multicomponent fiber (Figure 2e, Frame 4; Figure 2f(III)).

Figure 3 shows confocal microscopy images of several multicomponent fiber types achievable by the MIPC process, and the corresponding polyelectrolyte (droplet and interface) patterns required to achieve the respective fibers. Multicolored quantum dots (QDs) were found to be the ideal labels for differentiating the different components in each fiber. As anticipated from Figure 1c, each component appeared as a parallel compartment within the fiber, and the spatial arrangement of the different components corresponded to the polyelectrolyte pattern used. One primary rule was established for all the multicomponent fibers derived via the MIPC process – each component was derived from one nascent fiber arising from one interface. Thus, a two-interface MIPC yielded two nascent fibers and therefore, a two-component fiber (Figure 3a); while a four-interface MIPC yielded four nascent fibers and a four-component fiber (Figures 3b,d). In Figure 3b, the four-interface MIPC appears to have produced a three-component fiber, as reflected by the three different colors in the fiber; actually, the resulting fiber was a four-component fiber where two of the components were of the same color (red), overlapping in a linear fashion to produce the appearance of a single-colored domain.

The attractiveness of the MIPC process to produce multicomponent fibers is immediately apparent when the encapsulated components are biological entities, especially cells. **Figure 4** shows examples of various multicomponent fibers designed to contain specific cells within spatially defined domains. In Figure 4a, pre-osteoblast (MC-3T3) cells were encapsulated to form two layers that flanked a middle cell-free layer, employing the linear four-interface configuration depicted in Figure 3b. After a period of 72 h, the MC-3T3 cells have proliferated and aggregated within their respective domains (Figure 4b). Figure 4c shows a similar multicomponent configuration, but this time, two hepatocyte layers were encapsulated to flank a central endothelial cell (human umbilical vein endothelial cell (HUVEC)) layer. Such a configuration was chosen for its biomimetic significance–in native liver, parallel sheets of hepatocytes are closely associated

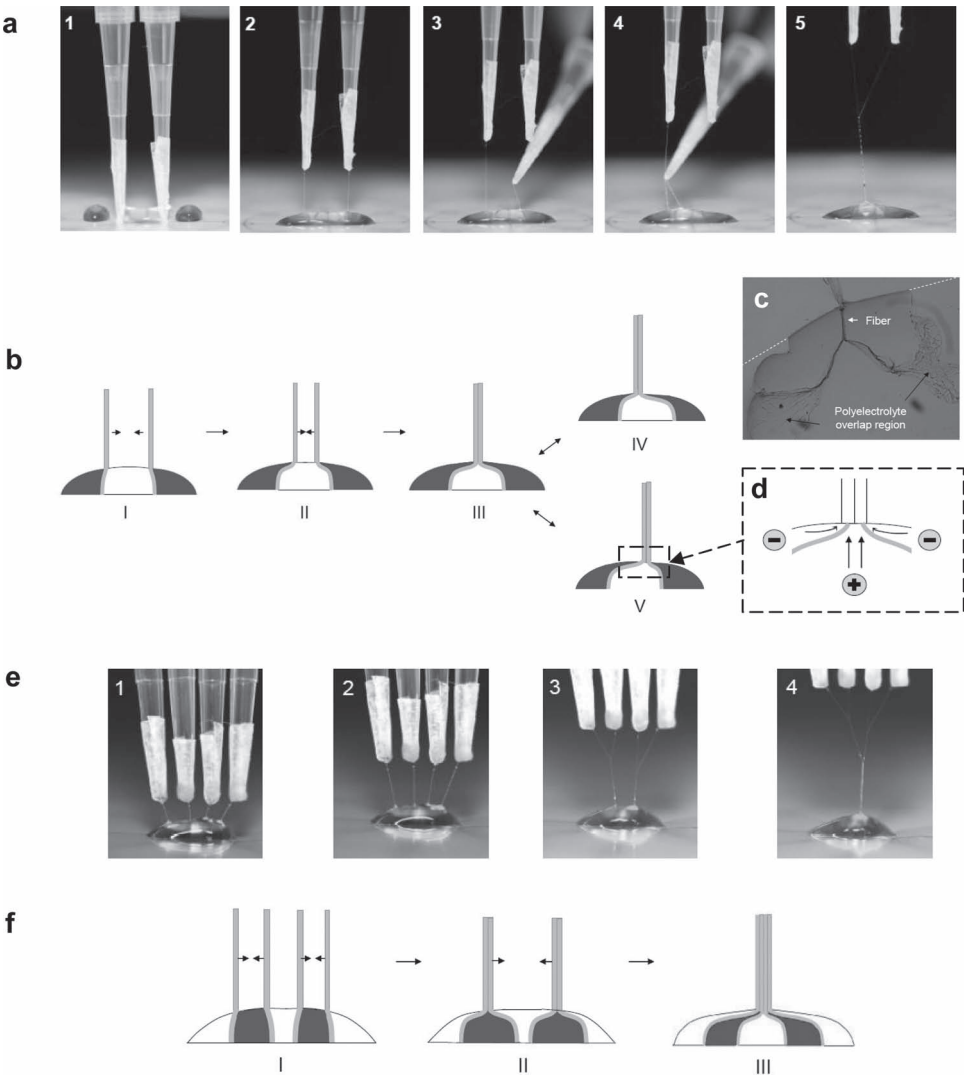

Figure 2. a) Still photographs and b) schematic drawing of a MIPC fiber drawing process involving two interfaces, leading to a two-component fiber. Polyanion: 1% sodium alginate solution colored with a blue food dye; polycation: 0.5% chitosan solution. c) Image of a dried MIPC assembly reveals a polyelectrolyte overlap region where the flanking polyelectrolytes overlap with the central polylectrolyte. d) Streaming of the central polyelectrolyte solution to the interface to replenish the consumed solution results in a constant layer of the latter interceding between the flanking polyelectrolyte solutions. e) Still photographs and f) schematic drawing of a MIPC fiber drawing process involving four interfaces. Sequential fusion of nascent fiber pairs leads to a four-component fiber.

with a central endothelium, and geometrically defined interactions between these cells have been established to be essential for liver function.[15] After two days of culture in vitro, endothelial tube structures were noted throughout the fiber structure, and the hepatocytes were observed to form aggregates in close association with these structures (Figures 4c,d).

Figure 4e demonstrates how three cell types can be simultaneously patterned within a fiber, using the triangular three-interface pattern depicted in Figure 3c. Parallel rows of the three cell types (labeled with different colors) could be discerned, which partially overlapped each other. Figure S4 (Supporting Information) shows an identical fiber configuration containing the same cell types, with cells being labeled with a Live–Dead assay. The results demonstrated that cells could be patterned with excellent viability within the fiber.

The ability to form a multicomponent fiber where the variable component was the extracellular matrix (ECM) and not cells suggested the possibility of creating "niche" microenvironments within a fiber, whereby each niche would contain a different combination of microenvironmental factors, e.g., matrix proteins or growth factors, which would influence the stem cell population housed within that niche accordingly. Thus, the linear two-interface configuration (Figure 3a) was used to construct a two-component fiber. Collagen type I was incorporated into one, but not the other component of the fiber, while human mesenchymal stem cells (hMSCs) were encapsulated into both. Figure 4f shows the appearance of the cells in the fiber after five days of culture. Stem cells on one-half of the fiber have spread and stretched along the axis of the fiber, whereas cells on the adjacent half remained rounded and formed clusters. Clearly,

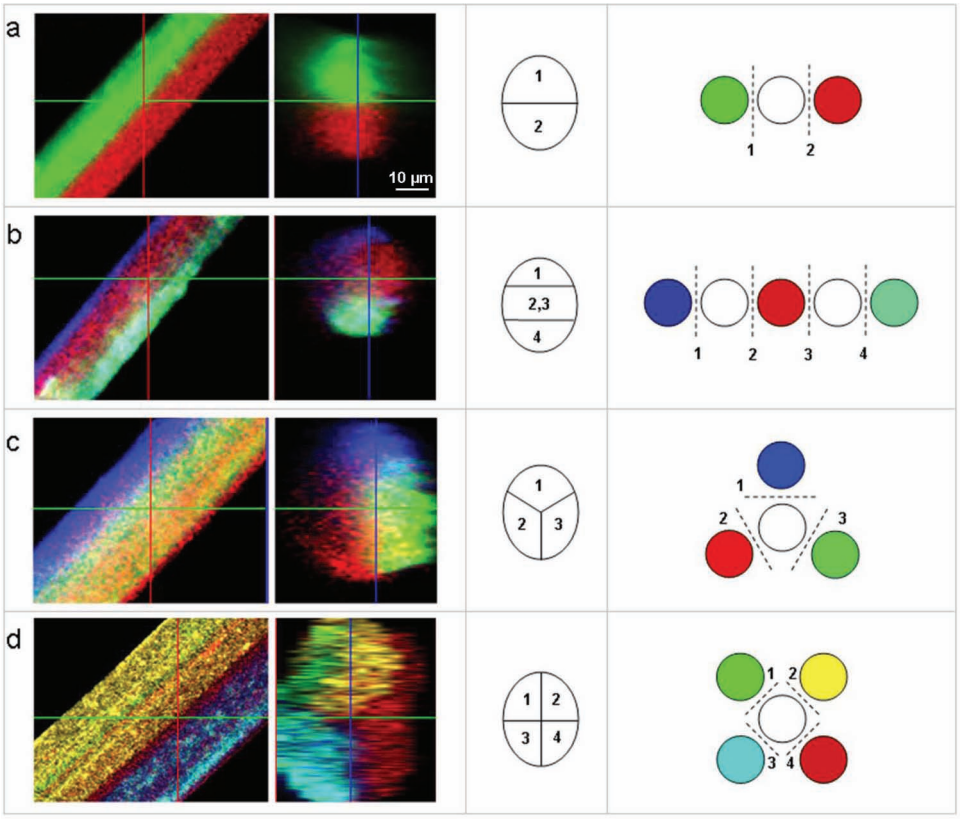

Figure 3. Multicomponent fibers obtained from MIPC involving a) two interfaces, b) four interfaces (linear configuration), c) three interfaces (triangle configuration), and d) four interfaces (square configuration). From left to right: Side-view image, cross-sectional image, schematic representation, and the corresponding polyelectrolyte droplet and interface (dashed line) patterns used for fiber drawing.

the half of the fiber that accommodated the elongated cells was the one that contained collagen, providing binding sites for the cells to attach and spread.[12,13]

In conclusion, a new phenomenon of MIPC has been described, leading to the formation of multicomponent fibers. The various components were spatially distributed within the fiber as parallel domains, in accordance with the droplet pattern used to generate the fiber. The usefulness of the multicomponent fibrous materials for 3D patterned co-culture of cells was illustrated by the encapsulation of various cell types in desired patterns. These experiments demonstrated cell migration, assembly and spreading within the fibers, and how these behaviors related to cell patterning. MIPC offers a technique that can ultimately lead to tissue constructs of higher complexity and function. It is anticipated that MIPC fibers would find significant value in biomedical applications, particularly as model systems for cell biology and as basic units for the engineering of human tissues and organs.

Experimental Section

Materials: For MIPC fiber drawing, 1% sodium alginate (low viscosity, Sigma) was typically used as the polyanion, while 0.5 w/v% chitosan (high MW, Aldrich) solution in 2% acetic acid (AR grade, Merck) or 1% water-soluble chitin (WSC) in 1× PBS was typically used as the polycation. WSC was prepared by a procedure modified from Takanori et al.[19] CellTracker Blue, Green and Red were purchased from Invitrogen (Singapore) and used according to manufacturer's instructions. Methylated collagen was prepared from Type I rat tail collagen (BD Biosciences) as described by Chia et al.[20] Briefly, the collagen was first precipitated using acetone, and vacuum dried. The methylation reaction was conducted by stirring the precipitated collagen in acidified methanol at room temperature for 24 h, followed by dialysis at room temperature for 24 h. The solution was then freeze dried to obtain the methylated product.

Cell Culture: HUVECs, NIH/3T3 fibroblasts, and HepG2 hepatocellular carcinoma cells were purchased from ATCC (USA). hMSCs were purchased from Lonza (Singapore). Primary rat hepatocytes were harvested from rat cadaver according to a previous report.[20] High-glucose Dulbecco's modified eagle medium (DMEM), hepatozyme-SFM, fetal bovine serum (FBS), GlutaMAX, and EndoGro-LS were purchased from Millipore (Singapore). Mesenchymal stem cells growth medium (MSCGM) and liquid penicillin-streptomycin (P/S) (10 kU, 100×) were purchased from Lonza (Singapore).

Multicomponent Fibers: Polyelectrolyte solutions of volume ranging from 5–20 μL were dispensed according to the droplet patterns depicted in Figure 3. The droplets were then brought into contact with one another to form stable interfaces (location shown as dashed lines in Figure 3). A pipette tip assembly, where the number of tips equaled to the number of interfaces, was positioned in relation to the polyelectrolyte droplets, such that each tip came into contact with one interface. Subsequently, the tips were drawn upwards at a rate of 0.4 mm s^{-1}. One nascent fiber was drawn from each interface, and all the nascent fibers were (manually or spontaneously) fused to form a single fiber. The drawing of multicomponent fibers is shown in Figures 2a and e for the cases of two interfaces and four interfaces, respectively.

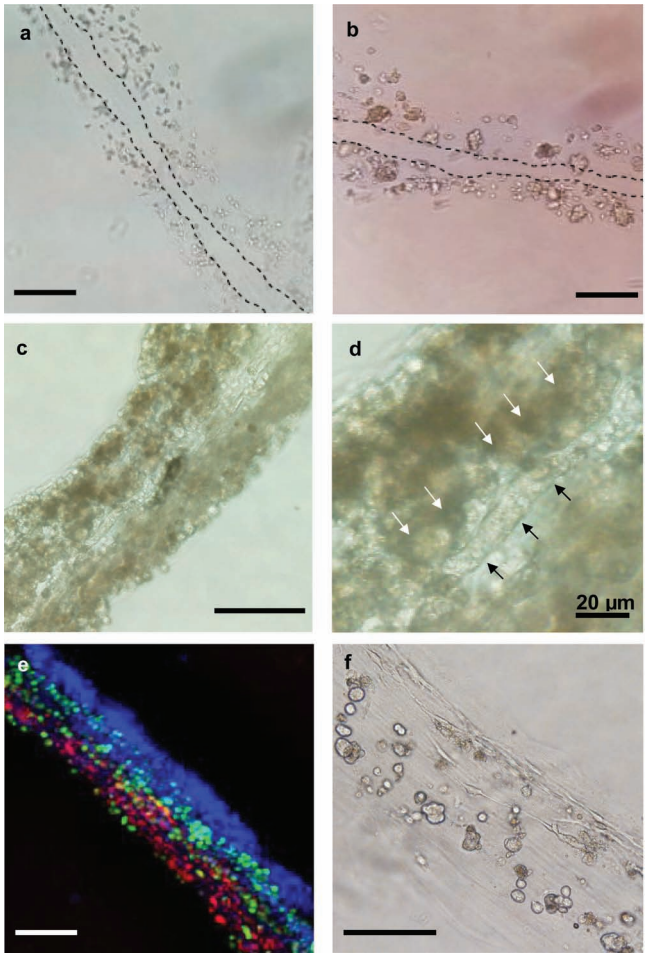

Figure 4. Cell encapsulation and patterning within multicomponent MIPC fibers. Two MC-3T3 cells layers flanking a cell-free domain: a) Day 0. b) Day 3. c–d) Two primary hepatocyte cell layers flanking a HUVEC layer at Day 2. Black arrows indicate an endothelial tube, and white arrows indicate the hepatocyte aggregates. e) Confocal microscopy image of three cell types within a three-component fiber: red – HUVEC, blue – fibroblast cells (NIH/3T3), green – HepG2. f) hMSCs cultured in a two-component fiber, one component with, and the other without collagen. Cell elongation and spreading are observed for cells in the collagen-containing half. WSC and alginate were used as the polycation and polyanion, respectively. Scale bar = 100 μm, unless otherwise indicated.

Encapsulation of Materials in Fiber: QDs were prepared as described in Supporting Information S5.[21] QDs were incorporated into multicomponent fibers by mixing the individually colored QDs (red, green, blue or yellow) into the different polyelectrolyte solutions prior to drawing. Cells were encapsulated by first centrifuging the cells down at a speed of 500 rpm for 3 min, then adding a specified volume of the desired cell type from the pellet to a volume of 1% WSC in PBS to obtain the desired cell density. Typically, 3 μL of a MC-3T3 pellet was added to 30 μL of PBS containing 1% WSC and 0.25% rat methylated collagen (RMC), 17 μL of a primary hepatocyte pellet was added to 30 μL of PBS containing 1% WSC and 0.25% RMC, and 20 μL of a HUVEC pellet was added to 20 μL of PBS containing 1% WSC and 0.25% RMC. Immediately upon the encapsulation of cells in the fibers, the latter were transferred to culture media suitable for culturing the cell type(s) concerned.

Supporting Information

Supporting Information is available from the Wiley Online Library or from the author.

Acknowledgements

The authors thank T. M. Hsieh for providing the primary rat hepatocytes and staff of the Biopolis Shared Facilities for confocal microscopy. Funding was provided by the Institute of Bioengineering and Nanotechnology (Biomedical Research Council, Agency for Science, Technology and Research (A*STAR), Singapore). J.K.C.T would like to thank A*STAR Graduate Academy for his graduate scholarship.

Received: October 10, 2011
Published online: December 16, 2011

[1] R. M. Fuoss, H. Sadek, *Science* **1949**, *110*, 552.
[2] A. S. Michaels, R. G. Miekka, *J. Phys. Chem.* **1961**, *65*, 1765.
[3] G. Decher, J. D. Hong, J. Schmitt, *Thin Solid Films* **1992**, *210/211*, 831.
[4] H. Yamamoto, Y. Senoo, *Macromol. Chem. Phys.* **2000**, *201*, 84.
[5] A. C. A. Wan, E. K. Yim, I. C. Liao, C. Le Visage, K. W. Leong, *J. Biomed. Mater. Res. A* **2004**, *71*, 586.
[6] I. C. Liao, A. C. A. Wan, E. K. Yim, K. W. Leong, *J. Control. Release* **2005**, *104*, 347.
[7] B. C. U. Tai, C. Du, S. J. Gao, A. C. A. Wan, J. Y. Ying, *Biomaterials* **2010**, *31*, 48.
[8] S. H. Lim, I. C. Liao, K. W. Leong, *Mol. Ther.* **2006**, *13*, 1163.
[9] S. Razdan, P. Patra, S. Kar, L. Ci, R. Vajtai, A. Kukovecz, I. Kiricsi, Z. Konya, P. M. Ajayan, *Chem. Mater.* **2009**, *21*, 3062.
[10] A. C. A. Wan, B. C. U. Tai, K.-J. Leck, J. Y. Ying, *Adv. Mater.* **2006**, *18*, 641.
[11] K. Narayanan, K.-J. Leck, S. Gao, A. C. A. Wan, *Biomaterials* **2009**, *30*, 4309.
[12] E. K. Yim, A. C. A. Wan, C. Le Visage, I. C. Liao, K. W. Leong, *Biomaterials* **2006**, *27*, 6111.
[13] S. Z. Yow, C. H. Quek, E. K. F. Yim, C. T. Lim, K. W. Leong, *Biomaterials* **2009**, *30*, 1133.
[14] D. A. Narmoneva, R. Vukmirovic, M. E. Davis, R. D. Kamm, R. T. Lee, *Circulation* **2004**, *110*, 962.
[15] S. N. Bhatia, U. J. Balis, M. L. Yarmush, M. Toner, *The FASEB Journal* **1999**, *13*, 1883.
[16] W. Tan, T. A. Desai, *J. Biomed. Mater. Res. A* **2005**, *72A*, 146.
[17] K. Nakao, R. Morita, Y. Saji, K. Ishida, Y. Tomita, M. Ogawa, *Nat. Methods.* **2007**, *4*, 227.
[18] A. C. A. Wan, I. C. Liao, E. K. Yim, K. W. Leong, *Macromolecules* **2004**, *37*, 7019.
[19] S. Takanori, K. Keisuke, I. Yoshio, *Makromol. Chem.* **1976**, *177*, 3589.
[20] Y. Du, S. M Chia, R. Han, S. Chang, H. Tang, H. Yu, *Biomaterials* **2006**, *27*, 5669.
[21] Y. Zheng, Z. Yang, Y. Li, J. Y. Ying, *Adv. Mater.* **2008**, *20*, 3410.